The shuffling rotation of the Earth's inner core revealed by earthquake doublets

Hrvoje Tkalčić[1]*, Mallory Young[1], Thomas Bodin[2], Silvie Ngo[1] and Malcolm Sambridge[1]

Geodynamical models and seismic observations suggest that the Earth's solid inner core rotates at a different rate than the mantle. However, discrepancies exist in rotation rate estimates based on seismic waves produced by earthquakes. Here we investigate the inherent assumption of a constant rotation rate using earthquake doublets—repeating earthquakes that produce similar waveforms. We detect that the rotation rate of the Earth's inner core with respect to the mantle varies with time. We perform an inverse analysis of 7 doublets observed at the College station, Alaska, as well as 17 previously reported doublets, and reconstruct a history of differential inner-core rotation between 1961 and 2007. We find that the observed doublets are consistent with a model of an inner core with an average differential rotation rate of 0.25–0.48° yr^{-1} and decadal fluctuations of the order of 1° yr^{-1} around the mean. The decadal fluctuations explain discrepancies between previous core rotation models and are in concordance with recent geodynamical simulations.

The differential rotation of the solid inner core with respect to the mantle emerges in geodynamo modelling, but its strength and direction is very sensitive to the imposed viscous boundary conditions at the inner-core boundary[1–4] and the balance between the gravitational and electromagnetic torques[5]. The discovery of systematic variations over time in travel times of inner-core-sensitive PKPdf waves[6] (Fig. 1c) from South Sandwich Islands (SSI) earthquakes observed in Alaska confirmed geodynamical predictions about the differentially rotating inner core. The estimated rotation rate of about 1.1–3° yr^{-1} in the eastward (prograde) direction[6,7] (Supplementary Fig. S1a) relied on the assumption that the fast axis of cylindrical anisotropy is tilted with respect to the Earth's rotation axis. However, since these initial studies, both the assumption that the direction of the fast axis of anisotropy can be uniquely determined and the assumption that a cylindrical anisotropy prevails in the inner core have been disputed[8,9] (see also refs 10,11).

Another method of detecting a differential rotation of the inner core abandoned the need for uniform cylindrical anisotropy[12]. According to this method a fixed source–receiver path will sample a volume of the inner core with increasing velocity as a function of time as the inner core spins with a different rate than the mantle, causing PKPdf waves of more recent earthquakes to traverse the inner core faster (Supplementary Fig. S1b). The obtained differential rotation was about 0.3° in the eastward direction. These results were criticized on the grounds that there are significant uncertainties in the earthquake location parameters, and that the contribution to travel times from short-scale inhomogeneities in the crust and mantle is significant in comparison with the resulting time shift in the PKPdf arrival[13]. A subsequent joint inversion for inner-core rotation and mantle heterogeneity confirmed a very robust lateral velocity gradient in the inner core and found an eastward differential rotation of between 0.3 and 1.1° yr^{-1} (ref. 14). This result was contrasted, however, by a study of earthquakes from 1977 to 1998, which found small temporal variations in the splitting functions of the normal modes sensitive to the Earth's core indicating a low differential rotation rate of 0.13±0.11° yr^{-1} (ref. 15).

The discrepancy between the body wave and normal mode results seems to reflect an inherent difficulty in obtaining accurate estimates of inner-core rotation. However, it may also indicate that the underlying assumption of a steady differential inner-core rotation is incorrect. If one instead allows for a time-variable inner-core rotation, different studies sampling different time intervals would be expected to yield different rotation rates. In fact, decadal fluctuations in inner-core rotation are indeed expected on geodynamical grounds. Detected decadal changes in the length of day (LOD) reflect the presence of time-dependent zonal flows in the fluid core[16,17]. Through electromagnetic coupling, these flows should entrain time-dependent variations in inner-core rotation with respect to the mantle. The more recent geodynamo models[18] suggest the presence of such fluctuations.

Earthquake doublets

Similar waveforms from earthquakes originating in the SSI region and observed in Alaska were first reported and used to question a prograde rotation of the Earth's inner core[19]. The use of earthquake doublets[20] offered a way to overcome the earlier problem of location errors and small-scale heterogeneities contaminating travel times. Earthquake doublets are repeating earthquakes that produce highly similar waveforms. The similarity in their waveforms attests that the waves initiated at the same location and traversed through the same Earth structure. In practice, this means that the separation of the two sources is smaller than the typical wavelength at which the waveforms are observed. Indeed, a recent relocation of the SSI earthquakes using improved algorithms verifies that they occur in tight spatial clusters[21]. Using a number of earthquake doublets, a significant and steady differential rotation of the inner core in the eastward direction was robustly determined to be about 0.4–1.0° yr^{-1} (ref. 20) and 0.3–0.5° yr^{-1} (ref. 22).

Here we present results of a new search for earthquake doublets using the College station (the station with the most complete continuous recording) and perform an analysis of their travel times. A common feature of all previous seismological studies using

[1]Research School of Earth Sciences, The Australian National University, Canberra, Australian Capital Territory 0200, Australia, [2]Berkeley Seismological Laboratory, University of California at Berkeley, Berkeley, California 94720, USA. *e-mail: Hrvoje.Tkalcic@anu.edu.au
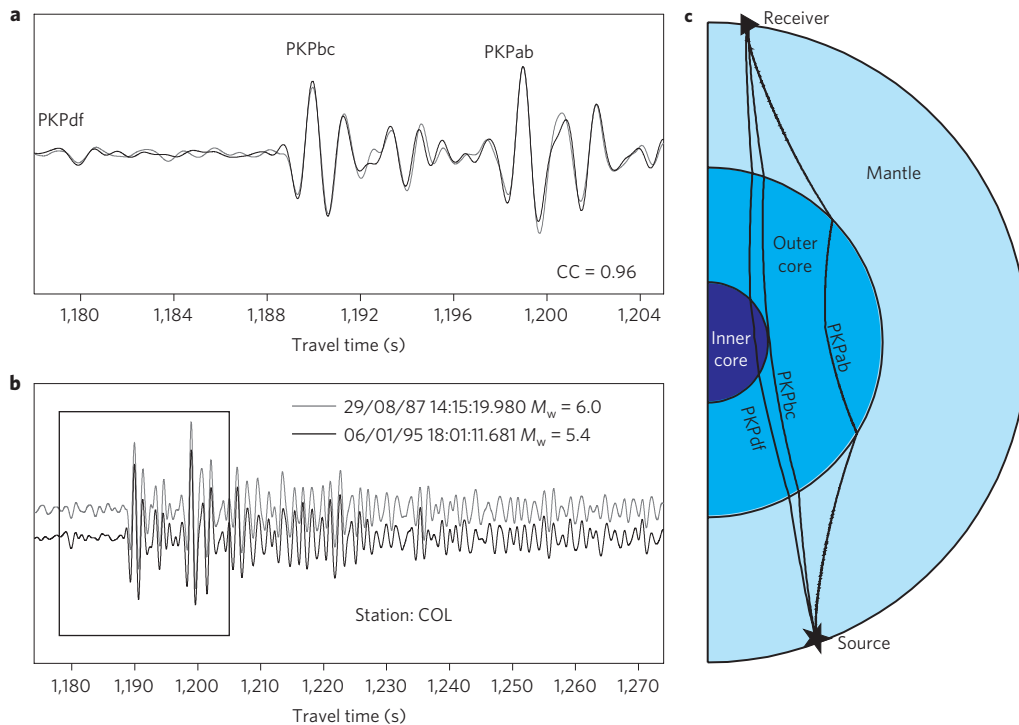
Figure 1 | Newly observed doublet and PKP waves. A newly observed doublet at the College station, Alaska (doublet #11; Supplementary Table S1; row 11). A more recently recorded waveform (6 January 1995) is shown in black. **a**, 3 branches of PKP waveforms enlarged from the rectangle in **b**. Cross-correlation coefficient CC between the two waveforms is shown in the lower right. **b**, Traces are aligned on the PKPbc phase and filtered between 0.5 and 1.0 Hz. Supplementary Fig. S8 gives more details about this doublet. **c**, A schematic representation of Earth's cross-section with ray paths of seismic waves referred to in this study; PKPdf, PKPbc and PKPab, shown. Note that only PKPdf waves traverse the Earth's inner core.

earthquake doublets was the assumption that the rate of inner-core differential rotation is constant with time. Using data less reliable than earthquake doublets, evidence for a fluctuation in the inner-core rotation rate has been found from a statistical-based spectral analysis[23] and an event pair travel time analysis[24]. Furthermore, a non-zero acceleration has been suggested for the past 55 years (ref. 25). On the basis of new earthquake doublet data and a new analysis technique, we show that a model with a non-steady rotation of the inner core with respect to the mantle is a plausible alternative to a steady-rotation model.

Difficulties associated with searching for doublets are escalated by the fact that most seismic stations of interest do not have continuous records (see Supplementary Methods). We design an algorithm to systematically search for repeating earthquakes originating in the South Sandwich Islands region. We first search for duplicates in P-waves recorded at the closest available stations, mostly in Antarctica. The waveforms recorded at the Antarctic stations are often complex owing to a high noise level, concealing potential earthquake doublets. In addition, the pairs of stations selected to confirm doublets do not always record common events (see Supplementary Methods S1.1). Despite this limitation, we observe 12 new doublets that were not reported in an earlier study of doublets[22], and we analyse 7 of them together with 17 previously reported doublets. The PKPdf waveforms of five doublets are too noisy for further analysis. One of the newly observed doublets is shown in Fig. 1a,b. A cross-correlation coefficient of 0.96 indicates high similarity of the waveforms. Only a small shift in PKPdf onsets was obtained for this doublet (0.05 ± 0.04 s) despite the time lapse of more than 7 years. The waveforms of all 24 doublets are shown in Fig. 2a. The traces shown are shifted so that the onsets of the PKPdf arrival of the earlier event of each doublet are roughly aligned. Several previously reported and new doublets are featured in Supplementary Figs S3–S10.

Variable rates of inner-core rotation

A linear, non-zero fit for all PKPdf time shifts as a function of time lapse would imply a constant rate of inner-core differential rotation with respect to the mantle over the past five decades. From Supplementary Figs S12–S14, however, it becomes clear that the PKPdf time shifts could be better explained if a time-variable rotation rate is allowed. For example, doublets #8 and #9 have similarly long time lapses of slightly more than 6 years, but the PKPdf time shift for doublet #8 is more than 0.2 s larger (Supplementary Fig. S13). In simple terms, this means that a pronounced change in the inner-core rotation rate is likely to have occurred between years 2002 and 2005.

Rather than imposing a linear fit to the PKPdf time shifts, we instead use a transdimensional Bayesian approach to invert for the expected slope and its change in time. This is an ensemble inference approach, where many potential solutions are generated with a variable number of unknowns using the reversible jump Monte Carlo algorithm[26–29]. For example, we used receiver functions and surface wave dispersion to invert for shallow Earth structure and demonstrated that it is possible to let the data infer the appropriate level of complexity in the recovered solution model[30]. Following a similar approach, the time interval here is divided into a variable number of B-splines, whose number and position of nodes along the time axis are unknowns in the algorithm (see Supplementary Methods S1.7 and Fig. S15).

With such a transdimensional formulation, the number of unknowns itself becomes an unknown in the inversion[30–32]. We first demonstrate that a transdimensional parametrization with an unknown number of B-splines is preferable to simple linear regression when inverting for the expected slope and its change with time (Supplementary Figs S14–S18). The root-mean-square of the best-fitting linear function (Supplementary Fig. S14) is 0.073 s, whereas the same value from the expected average cubic
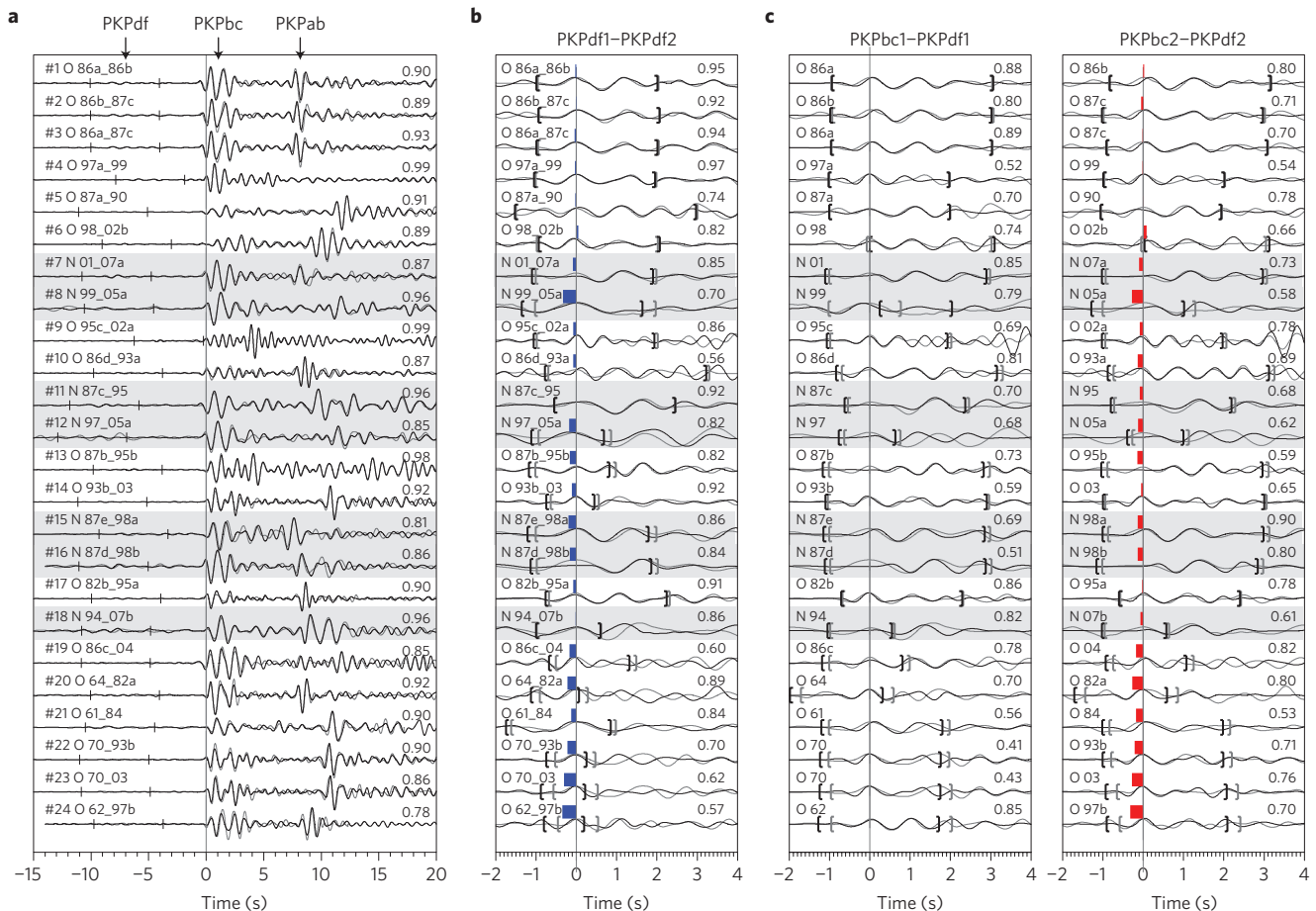
Figure 2 | Waveform doublets and measurement methods. a, PKP waveforms observed at College station, Alaska for 24 doublets originating from the SSI region. Seventeen doublets were discovered previously[22] (marked by O for old) and seven new doublets are reported in this study (grey shade; marked by N for new). The traces (grey for the earlier events and black for the later events) are aligned with the PKPbc phase and sorted with increasing time separation from top to bottom. **b**, Method 1: enlarged PKPdf segments for each doublet marked by ticks in **a**. The bracketed segments are aligned using cross-correlation. Blue horizontal bars indicate the measured PKPbc–PKPdf travel-time difference. **c**, Method 2: enlarged PKPdf and PKPbc segments of the first event of a doublet (left) and the second event of a doublet (right). The traces indicated by brackets are aligned using cross-correlation. Red horizontal bars indicate the measured PKPbc–PKPdf travel-time difference.

splines model (shown in Fig. 3a) is 0.047 s, thus indicating a significantly better fit to the data. Figure 3a (red line) shows a solution averaged over 300,000 samples. The variation of the time differences curve is complex, with the most probable increases in slope occurring during the late 1960s, the early 1990s and between 2002 and 2004 (Figs 3a and 4a). The most probable significant decreases occur during the late 1970s, the late 1990s and after 2004. Here the uncertainty on each doublet measurement is assumed to be inversely proportional to the cross-correlation coefficient associated with that doublet. The posterior probability distribution for the number of nodes is given in Fig. 3b. Results of synthetic tests (Supplementary Figs S16–S18) further justify the use of a transdimensional Bayesian approach.

The fit shown in Fig. 3a can be differentiated and presented as a slope in $s\,yr^{-1}$ (Fig. 4a). Assuming a heterogeneity gradient in the inner core, the slope ($s\,yr^{-1}$) can be converted to an inner-core rotation rate ($°\,yr^{-1}$) using $\alpha = -\gamma\,\delta t/(\partial v/\partial L)$, where γ is a dimensionless correction factor relating the change in source–receiver distance to the change of azimuth, δt is the slope ($s\,yr^{-1}$) normalized by the total time PKPdf waves spend in the inner core ($\%,s\,yr^{-1}$), and $\partial v/\partial L$ is the lateral velocity gradient in the inner core obtained by previous workers[14] (between -0.0278% per degree without mantle structure corrections and -0.0145% per degree with mantle corrections). Figure 4b thus shows a

possible model for the recent history of the inner-core rotation rate determined by our study, which assumes a known velocity gradient. The model is characterized by a non-steady rotation of the inner core with respect to the mantle.

Reconciling rotation from body waves and normal modes

Differential travel times of PKP waves from the SSI recorded in Alaska have been previously used to observe temporal changes in PKPdf waves[12]. The time span of data in that study was from 1967 to 1996. Figure 4b shows that during that 30-year interval, the most pronounced increase in the inner-core rotation rate occurred during the late 1960s, according to our study. The rate climbed steeply to about 0.5–$1°\,yr^{-1}$ (depending on the structural model used) and then declined for approximately 10 years thereafter. There was another increase in the rotation rate in the late 1980s, which resulted in a deceleration and a return to a zero rate around 2000. We integrated the rotation rate over the time interval used in ref. 12 and obtained a cumulative shift in alignment of the inner core to the mantle of 8.48–16.26°, depending on whether mantle corrections[14] are included or not (Table 1). When divided by the total time interval, a resulting average rotation rate of 0.30–$0.58°\,yr^{-1}$ (with and without corrections for near-station structure) compares well to previous results[12]. Earthquake doublets that were analysed in ref. 22 encompassed the time interval of
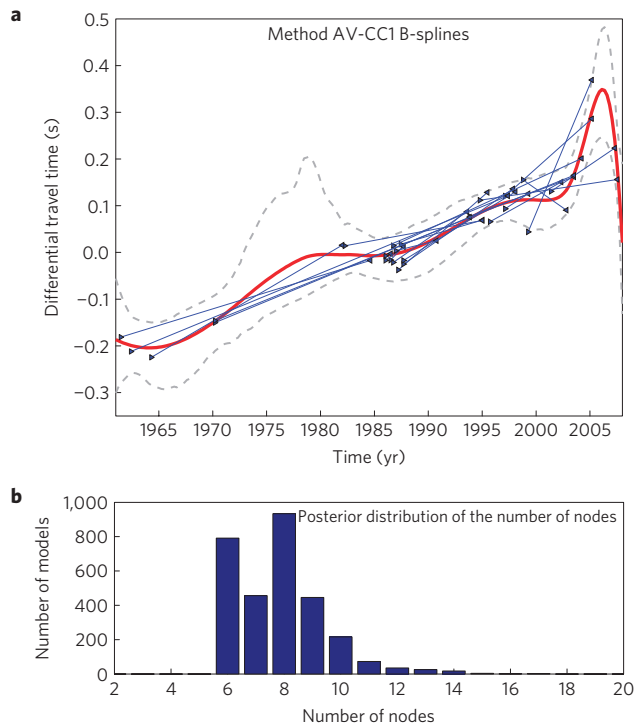
Figure 3 | Solution model and posterior distribution of the number of nodes. a, Doublet measurements (blue triangles represent measurements for each earthquake of a doublet and are joined with straight lines) are fitted with a variable slope model using a Bayesian transdimensional inversion derived as an average over the ensemble of collected models. The red line shows the expected solution model (normalized to zero mean). The dashed grey line is an average solution ±1 s.d. **b,** Posterior distribution for the number of B-spline nodes across the ensemble solution (Supplementary Sections S1.7 and S1.9).

Figure 4 | Inner-core differential rotation rate as a function of time. a, The slope parameter as determined by the inversion (Fig. 3). Blue areas indicate eastward rotation whereas red areas indicate westward rotation. **b,** Differential rotation rate as derived from the slope for three different values of the velocity gradient[14]. The dark grey and the light grey rectangles delineate the time intervals used in the study of doublets[22] and normal modes[15]. The areas under these curves were integrated to estimate the total shift (Table 1). The dashed line is the solution obtained when doublet #8 is omitted from the inversion.

1961–2004, 15 years longer in duration than that of the travel time study[12]. When the rotation rate is integrated and divided by the time interval of 1961–2004 (see dark grey rectangle in Fig. 4b), the obtained average rate is in good agreement with previously published results, yielding 0.31, 0.51 and 0.63° yr^{-1} in this study compared to 0.27, 0.43 and 0.53° yr^{-1} in ref. 22; compare the 1961–2004 doublets column of Table 1 with Supplementary Table S5 from ref. 22. After interpreting Fig. 4, it becomes clear that the larger differential rotation rate value compared with that obtained in the travel-time study comes from two further increases in the rotation rate: one occurring during the late 1960s and one occurring between 2002 and 2005. We note that during the 1971–1974
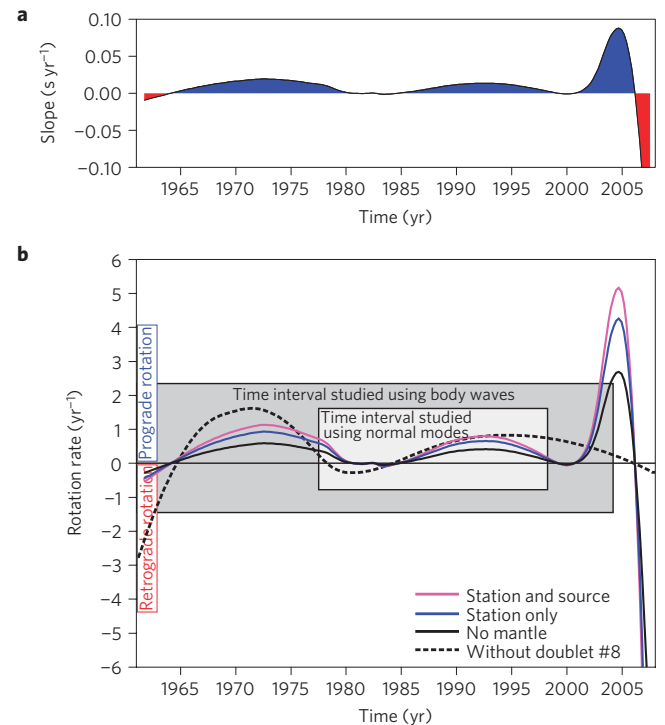
time interval a small inner-core rotation rate of 0.15° yr^{-1} was obtained from an independent study of scattering[33]. Although this time interval is relatively short, the high, however decelerating, inner-core rotation rates of 0.5–1° yr^{-1} of our model (Fig. 4) are in apparent disagreement with this scattering study.

Whereas body wave studies tend to be superior in revealing short-scale features, normal modes, although sensitive to inner-core differential rotation, are insensitive to small-scale heterogeneity and anisotropy. Figure 4 indicates that the rotation of the inner core in the time period 1977–1998 was characterized by acceleration starting after 1985 and deceleration starting before 1995, but for the rest of the time the rotation was close to zero with respect

Table 1 | Shifts in angular alignment between the inner core and the mantle and average shift rates over time.

Lateral gradient from ref. 14 with and without mantle correction (% per degree)	1967–1996 travel times[12]		1977–1998 normal modes[15]		1961–2004 doublets[22]		1961–2007 doublets, this study	
	Shift (°)	Shift/time (° yr^{-1})	Shift (°)	Shift/time (° yr^{-1})	Shift (°)	Shift/time (° yr^{-1})	Shift (°)	Shift/time (° yr^{-1})
−0.0278 no mantle corr.	8.48	0.30	4.10	0.19	13.27	0.31	11.43	0.25
−0.0176 station only	13.39	0.48	6.49	0.31	21.97	0.51	18.05	0.39
−0.0145 station and source	16.26	0.58	7.88	0.38	26.66	0.63	21.91	0.48

Integrated total shift in alignment of the inner core with respect to the mantle for time intervals from previous studies and for the entire time-interval sampled by the existing earthquake doublets. Different total shifts (°) were obtained for each time interval (associated with previous studies[12,15,22]) for three different lateral gradients in velocity[14]. Also shown is average shift over time (° yr^{-1}). Compare results from this table with Supplementary Table S5 from ref. 22.

to the mantle. Interestingly, the inner core underwent a slight westward rotation between the years 1981 and 1985. We integrated the rotation rate over a period of approximately 20 years (shown by light grey rectangle in Fig. 4b) and obtained a total shift of 4.10° (see the 1977–1998 normal modes column in of Table 1) when mantle correction are ignored. After dividing by the total time interval, we retrieved an average rate of 0.19° yr^{-1}, in agreement with normal modes from the same time interval[15]. Slightly higher values were obtained when the station and source corrections were applied (0.31 and 0.38° yr^{-1}). Overall, our averaged rate obtained from the normal modes time interval is significantly smaller than that resulting from the doublets time interval.

The above calculations thus provide a quantitative explanation for and an elegant resolution to the long-standing discrepancy between differential rotation rates derived from either body waves[6,12,14,20,22] or normal modes[15] alone (Fig. 4b; for the concept, see Supplementary Fig. S1c).

Geodynamical implications

Our results reveal that although at times the angular alignment of the inner core and the mantle remains negligibly small or even negative (retrograde rotation), the inner core exhibits cumulative rotation in the eastward direction (prograde rotation) with a mean rate of 0.25–0.48° yr^{-1}, depending on the Earth model used for travel time corrections (Table 1). This produces a total eastward shuffle between about 11 and 22° over the time interval of 1961–mid 2007 (Table 1). Our study provides an alternative to the steady-rotation model and suggests that superimposed on this average motion are decadal fluctuations. The most striking feature of the recovered differential rotation time history is the large fluctuation starting after 2000 characterized by a sharp acceleration and then a deceleration that leads to a retrograde rotation. Its magnitude is uncertain owing to the edge effects imposed by the B-spline parametrization and disappears completely when doublet #8 is excluded from the inversion, as shown by our bootstrap test (Fig. 4b and Supplementary Method S1.10 and Fig. S18). Although the error associated with doublet #8 is not larger than that of other doublets, further data are required to further constrain the inner-core rotational dynamics for these more recent years. In the meantime, a more conservative model should be considered (dashed line in Fig. 4b) while noting that the exclusion of doublet #8 does not change the main conclusions about the shuffling rotation of the inner core.

Present constraints on the amplitude of fluctuation in the differential rotation rate of the inner core are based on LOD variations not exceeding those observed. These constraints depend on the assumptions about the relative strength of electromagnetic coupling at the core–mantle boundary and gravitational coupling. In a previous study[34], the inner-core–mantle gravitational coupling strength was required to be quite large to explain the 6 yr mode in LOD. However, a more recent study[35] suggests a different source for this mode, thereby making a weaker gravitational coupling strength viable. When inner-core differential rotation is approached from an angular momentum perspective as in ref. 36, a rate of about 0.25° yr^{-1} at all periods of fluctuation does not violate the observed LOD so long as the product of Γ and τ is smaller than 5×10^{19} N m yr, where Γ is the gravitational coupling factor and τ is the viscous relaxation time of the inner core. Keeping in mind the uncertainties in estimates of electromagnetic coupling at the core–mantle boundary[36], the observed inner-core fluctuations shown in Fig. 4b can be used to place upper bounds on the gravitational coupling.

Although other mechanisms, such as variable inner-core topography[37,38] or rapidly changing structure in the inner or outer core[39], have been suggested to explain seismic observations, the inferred acceleration of the inner core is in agreement with

geodynamical simulations. Using a torque balance equation such as in ref. 18 and a previous gravitational torque estimate[36], the exciting electromagnetic torque required to explain the observed accelerations in our model of inner-core rotation is ∼1.19 × 10^{20} N m, which agrees with published values[5].

Recent numerical geodynamo simulations suggest that present-day seismically inferred mean rotation rates of several tenths of a degree per year could be a fragment of a time-varying signal rather than a steady super rotation[18]. If, one the one hand, the mantle has a major influence on the core dynamics, it would take a very slow rotation of 1° Myr^{-1}, assuming an inner core growth rate of 1 mm yr^{-1} (ref. 40), to preserve a degree-one longitudinal signature at the top 100 km of the inner core, as seismological evidence suggests there exists[41,42]. We note that despite attempts to map the slow to fast transition as a function of depth[43], the present core-sensitive seismological data do not provide dense enough spatial sampling to constrain a sharp transition from the slow to the fast hemisphere of the inner core. If, on the other hand, the core dynamics are minimally influenced by the mantle, a development of a hemispherical structure at the top of the inner core is possible through a much faster dynamical mechanism, such as degree-one convection[44,45].

Methods

We measure PKPdf travel-time differences between the first and the second event of a doublet using the approach described in ref. 22 (Method 1). After the waveforms of two earthquakes forming a doublet are aligned on the PKPbc arrivals (see Supplementary Figs S4, S6, S8 and S10; top panel), we cross-correlate the PKPdf waveforms and obtain the same or very similar results to those reported in ref. 22 (compare columns 4 and 5 of Supplementary Table S1). The waveforms before and after the time shift are shown in the middle panel of Supplementary Figs S4, S6, S8 and S10. The cross-correlation coefficients indicate the similarity of waveforms for both long waveform sections (showing the quality of a doublet) and small sections around the PKPdf waves (showing the quality of an individual measurement). They are either comparable to or slightly higher than those previously reported (Supplementary Methods S1.3). The obtained PKPdf time shifts using Method 1 are shown with blue bars in Fig. 2b and column 5 of Supplementary Table S1. The time shifts obtained by an alternative method (Method 2) are shown with red bars in Fig. 2c and are reported in column 6 of Supplementary Table S1. In Method 2, we measure the PKPbc–PKPdf differential travel time for each of the two earthquakes in a doublet and subtract one from the other to get the desired time shift of PKPdf waves. The waveforms corrected for the time shift are shown in the bottom left panel of Supplementary Figs S6–S29. We take the average PKPdf time difference obtained by method 1 and 2 as the measured time difference (also see discussion about method 3 and Supplementary Fig. S11).

We then perform a Bayesian inversion parameterizing the regression model with a variable number of cubic B-splines. The solution is not a single best-fit model, but a large ensemble of models that are distributed according to the posterior probability density function. The likelihood (the probability of the data d given the model m) is defined by a least-squares misfit function given by the distance between observed and estimated data:

$$p(d|m) = \frac{1}{\prod_{i-1}^{N} \left(\sqrt{2\pi\sigma_i^2} \right)} \exp \left[\sum_{i=1}^{N} \frac{-(g(m)_i - d_i)^2}{2(\sigma_i)^2} \right] \quad (1)$$

where d_i is the data i, $g(m)_i$ is the data i estimated from a given model m, and σ_i is the standard deviation of an assumed random Gaussian noise for measurement i. In our problem, we do not know the number of cells; that is, the dimension of the model space is itself a variable, and hence the posterior becomes a transdimensional function.

The seismic waveform data used in this study were obtained from Incorporated Research Institutions for Seismology Data Management Centre (http://iris.edu).

Supplementary Sections S1.1–S1.11 provide a full description of waveform doublet identification, measurements, transdimensional Bayes analyses and validation.

References

1. Glatzmaier, G. H. & Roberts, P. H. Rotation and magnetism of Earth's inner core. *Science* **274,** 1887–1891 (1996).
2. Gubbins, D. Rotation of the inner core. *J. Geophys. Res.* **86,** 11695–11699 (1981).
3. Kuang, W. & Bloxham, J. An Earth-like numerical dynamo model. *Nature* **389,** 371–374 (1997).

4. Olson, P. Probing Earth's dynamo. *Nature* **389,** 337–338 (1997).
5. Aurnou, J. M. & Olson, P. Control of inner core rotation by electromagnetic, gravitational and mechanical torques. *Phys. Earth Planet. Int.* **117,** 111–121 (2000).
6. Song, X. & Richards, P. Seismological evidence for differential rotation of the Earth's inner core. *Nature* **382,** 221–224 (1996).
7. Su, W-J., Dziewonski, A. M. & Jeanloz, R. Planet within a planet: Rotation of the inner core of Earth. *Science* **274,** 1883–1887 (1996).
8. Su, W. J. & Dziewonski, A. M. A local anomaly in the inner core. *Eos Trans. AGU (Spring Meet. Suppl.)* **79,** S218 (1998).
9. Souriau, A., Roudil, P. & Moynot, B. Inner core differential rotation: Facts and artefacts. *Geophys. Res. Lett.* **24,** 2103–2106 (1997).
10. Souriau, A. in *Deep Earth Structure—The Earth's Cores, in Treatise on Geophysics* Vol. 1 (ed. Schubert, G.) 655–693 (Elsevier, 2007).
11. Tkalčić, H. & Kennett, B. L. N. Core structure and heterogeneity: A seismological perspective. *Austral. J. Earth Sci.* **55,** 419–431 (2008).
12. Creager, K. Inner core rotation rate from small-scale heterogeneity and time-varying travel times. *Science* **278,** 1284–1288 (1997).
13. Souriau, A. New seismological constraints on differential rotation of the inner core from Novaya Zemlya events recorded at DRV, Antarctica. *Geophys. J. Int.* **134,** F1–F5 (1998).
14. Song, X. D. Joint inversion for inner core rotation, inner core anisotropy, and mantle heterogeneity. *J. Geophys. Res.* **105,** 7931–7943 (2000).
15. Laske, G. & Masters, G. *Earth's Core: Dynamics, Structure, Rotation* Vol. 31 (eds Dehant, V. *et al.*) 5–21 (Geodymanics Series, American Geophysical Union, 2003).
16. Jault, D., Gire, C. & Le Mouel, J-L. Westward drift, core motions and exchanges of angular momentum between core and mantle. *Nature* **333,** 353–356 (1988).
17. Jackson, A., Bloxham, J. & Gubbins, D. *Dynamics of Earth's Deep Interior and Earth Rotation* Vol. 72 (eds Le Mouël, J-L., Smylie, D., & Herring, T.) 97–107 (Geophysical Monograph Series, American Geophysical Union, 1993).
18. Aubert, J. & Dumberry, M. Steady and fluctuating inner core rotation in numerical geodynamo models. *Geophys. J. Int* **184,** 162–170 (2011).
19. Poupinet, G., Souriau, A. & Coutant, O. The existence of an inner core super-rotation questioned by teleseismic doublets. *Phys. Earth Planet. Int.* **118,** 77–88 (2000).
20. Li, A. & Richards, P. G. Using earthquake doublets to study inner core rotation and seismicity catalog precision. *G-cubed* **4,** 1–23 (2003).
21. Bondár, I. & Storchak, D. Improved location procedure at the International Seismological Centre. *Geophys. J. Int.* **186,** 1220–1244 (2011).
22. Zhang, J., Song, X. D., Li, Y., Richards, P. G. & Sun, X. Inner core differential motion confirmed by earthquake waveform doublets. *Science* **309,** 1357–1360 (2005).
23. Collier, J. D. & Hellfrich, G. Estimate of inner core rotation rate from United Kingdom regional seismic network data and consequences for inner core dynamical behaviour. *Earth Planet. Sci. Lett.* **193,** 523–537 (2001).
24. Song, X. & Poupinet, G. Inner core rotation from event-pair analysis. *Earth Planet Sci. Lett.* **261,** 259–266 (2007).
25. Lindner, D., Song, X., Ma, P. & Christensen, D. H. Inner core rotation and its variability from nonparametric modeling. *J. Geophys. Res.* **115,** B04307 (2010).
26. Denison, D. G. T., Holmes, C., Mallick, B. & Smith, A. F. M. *Bayesian Methods for Nonlinear Classification and Regression* (Wiley, 2002).
27. Geyer, C. & Møller, J. Simulation procedures and likelihood inference for spatial point processes. *Scand. J. Statist.* **21,** 359–373 (1974).
28. Green, P. Reversible jump MCMC computation and Bayesian models selection. *Biometrika* **82,** 711 (1995).
29. Green, P. Trans-dimensional Markov chain Monte Carlo. *Highly Struct. Stocha. Syst.* **27,** 179–198 (2003).
30. Bodin, T., Sambridge, M., Tkalčić, H., Gallagher, K. & Arroucau, P. Transdimensional inversion of receiver functions and surface wave dispersion. *J. Geophys. Res.* **117,** B02301 (2012).
31. Bodin, T. & Sambridge, M. Seismic tomography with the reversible jump algorithm. *Geophys. J. Int.* **178,** 1411–1436 (2009).
32. Sambridge, M., Bodin, T., Gallagher, K & Tkalčić, H. Transdimensional inference in the geosciences. *Phil. Trans. R. Soc. A* **371,** 20110547 (2013).
33. Vidale, J. E. & Earle, P. S. Evidence for inner core rotation from possible changes with time in PKP coda. *Geophys. Res. Lett.* **32,** L01309 (2005).
34. Dumberry, M. Geodynamic constraints on the steady and time dependent inner core axial rotation. *Geophys. J. Int.* **170,** 886–895 (2007).
35. Gillet, N., Jault, D., Canet, E. & Fournier, A. Fast torsional waves and strong magnetic field within the Earth's core. *Nature* **465,** 74–77 (2010).
36. Dumberry, M. & Mound, J. Inner core–mantle gravitational locking and the super-rotation of the inner core. *Geophys. J. Int.* **181,** 806–817 (2010).
37. Wen, L. Localized temporal change of the Earth's inner core boundary. *Science* **314,** 967–970 (2006).
38. Cao, A., Masson, Y. & Romanowicz, B. Short wavelength topography on the inner-core boundary. *Proc. Natl Acad. Sci. USA* **104,** 31–35 (2007).
39. Mäkinen, A. M. & Deuss, A. Global seismic body-wave observations of temporal variations in the Earth's inner core, and implications for its differential rotation. *Geophys. J. Int.* (2011).
40. Dumberry, M. Gravitationally driven inner core differential rotation. *Earth Planet. Sci. Lett.* **297,** 387–394 (2010).
41. Tanaka, S. & Hamaguchi, H. Degree one heterogeneity and hemispherical variation of anisotropy in the inner core from PKP(BC)-PKP(DF) times. *J. Geophys. Res.* **102,** 2925–2938 (1997).
42. Niu, F. & Wen, L. Hemispherical variations in seismic velocity at the top of the Earth's inner core. *Nature* **410,** 1081–1084 (2001).
43. Waszek, L., Irving, J. & Deuss, A. Reconciling the hemispherical structure of Earth's inner core with its super-rotation. *Nature Geosci.* **4,** 264–267 (2011).
44. Monnereau, M., Calvet, M., Mergerin, L. & Souriau, A. Loopsided growth of Earth's inner core. *Science* **328,** 1014–1017 (2010).
45. Alboussière, T., Deguen, R. & Melzani, M. Melting-induced stratification above the Earth's inner core due to convective translation. *Nature* **466,** 744–747 (2010).

Author contributions

S.N. and H.T. contributed algorithms and methods for doublet search. M.Y., S.N. and H.T. worked together on improving methods for identification of doublets and their measurements. M.Y. performed time measurements and made the waveform figures under the supervision and verification of measurements by H.T. The inversion approach was designed by T.B. based on his PhD thesis supervised by M.S. and discussions with H.T. Synthetic tests were designed by H.T. and T.B., and T.B. contributed figures and supplementary text related to the Bayesian method. H.T. designed the study, wrote the manuscript and produced the figures, which all authors commented on and edited.

Additional information

Supplementary information is available in the online version of the paper. Reprints and permissions information is available online at www.nature.com/reprints. Correspondence and requests for materials should be addressed to H.T.

Competing financial interests

The authors declare no competing financial interests.